Supporting Information for

Signal transductions of BEAS-2B Cells in response to carcinogenic $PM_{2.5}$ exposure based on microfluidic system

Authors: Lulu Zheng[1], Sixiu Liu[1]*, Guoshun Zhuang[1], Jian Xu[1], Qi Liu[1], Xinlian Zhang[1], Congrui Deng[1], Zhigang Guo[1], Wang Zhao[1], Tingna Liu[1], Yiqi Wang[1], Yuxiao Zhang[1], Jing Lin[1], Qiongzhen Wang[1] & Guodong Sui[1, 2]*

[1]Shanghai Key laboratory of Atmospheric Particle Pollution Prevention (LAP3), Department of Environmental Science & Engineering, Fudan University, 220 Handan Road, Shanghai 200433, P.R. China.

[2]Institute of Biomedical Science, Fudan University, Shanghai 200433, P.R.China.

Correspondence: Email: gsui@fudan.edu.cn; liusixiu@fudan.edu.cn

Supporting Information Contents:

1. Supplementary Materials and Methods

A. Site description

The sampling site is located on the roof of the No. 4 teaching building on main campus of Fudan University (31.3° N, 121.5° E), which is representative of a typical urban environment in Shanghai, including a mixture of residential, traffic, construction, and industrial sources. This observational site is approximately 40 km away from the East China Sea. The closest industrial sources are located approximately 10.5 km away and are primarily to the southeast and northwest[1]. Approximately 25 million residents live in this area (SMSB, 2011). Previous studies [2] confirmed this site as an ideal location for characterizing regional air pollution in the Yangtze River Delta).

B. Sampling

The $PM_{2.5}$ samples in spring (9 April-28 April 2012), summer (26 July-14 August 2012), Fall (27 October-16 November 2011) and winter (24 December 2011-9 January 2012) were collected on Whatman® 41 filters (Whatman Inc., Maidstone, UK) using a medium-volume sampler (Qingdao Hengyuan Science &Technology Development Co., Ltd.; model: HY-100 $PM_{2.5}$; flow rate: 6 m^3/h) for a consecutive period of 24 hours regularly started at 08:00 local time (UTC+8). Concurrently, another medium-volume sampler (Guangzhou Mingye Huanbao Technology Company; flow rate: 18 m^3/h) was used to collect $PM_{2.5}$ samples with pre-baked quartz filters (20×25 cm^2, 2500QAT, PALL, USA) to measure carbonaceous aerosols and PAHs in particulate phases. The samples were stored in a refrigerator prior to

analysis. The filters were weighed before and after sampling using an analytical balance (Model: Sartorius 2004 MP, reading precision 10 μg) after stabilizing under constant temperature (20 ± 1°C) and humidity (40 ± 1 %) in a chamber for over 48 h. All procedures were strictly quality controlled to avoid possible contamination of the samples.

C. Ion Analysis

One quarter of each sample and blank filter were extracted ultrasonically with 20 ml deionized water (18 MΩ cm^{-1}). Inorganic ions (Na^+, NH_4^+, K^+, Mg^{2+}, Ca^{2+}, SO_4^{2-}, NO_3^-, and Cl^-) were analyzed using Ion Chromatography (IC; Dionex ICS 3000, USA) with Dionex Ionpac AS 11 separation columns for anions and Dionex Ionpac CS 12A separation columns for cations in addition to guard columns (Dionex Ionpac AG 11), a self-regenerating suppressed conductivity detector (Dionex Ionpac ED50), and a gradient pump (Dionex Ionpac GP50). The procedures were described in detail elsewhere [3].

D. Element analysis

Half of each aerosol sample and the blank filters were digested at 180 °C for 30 min in a high pressure Teflon digestion vessel with 8 ml concentrated HNO_3 and 0.6 ml concentrated HF by a Microwave Accelerated Reaction System (MARS 5; CEM, USA). The solutions were dried and then diluted to 10 ml with 0.2 ml concentrated HNO_3 and deionized water (18 MΩ cm^{-1}). In total, 15 elements (Al, Fe, Mn, Ti, Ba, Ni, Cu, P, Pb, Co, Zn, Cd, V, Sr and As) were measured using an inductively coupled

plasma optical emission spectroscopy (ICP-OES; SPECTRO, Germany). The detailed analytical procedures are described elsewhere [4].

E. Carbonaceous aerosol analysis

OC and EC in $PM_{2.5}$ samples were detected by the IMPROVE thermal/optical reflectance (TOR) protocol [5] using the Thermal/Optical Carbon Analyzer (DRI Model 2001). For each sample, a 0.544 cm^2 area was punched to measure the eight carbon fractions (OC1, OC2, OC3, OC4 at 140 °C, 280 °C, 480 °C and 580 °C, respectively, in a helium atmosphere; EC1, EC2, EC3 at 580°C, 740 °C and 840 °C, respectively, in the 98 % helium/2 % oxygen atmosphere; and OP, optically detected pyrolyzed carbon). OC and EC were defined by the IMPROVE protocol as OC1 + OC2 + OC3 + OC4 + OP and EC1 + EC2 + EC3 - OP, respectively.

F. PAHs analysis

The analytical procedure of USEPA priority 16 PAHs has been described previously [1,6] Briefly, half of each quartz filter was used for Soxhlet extraction. All extracted samples were injected with hexamethylbenzene and then concentrated to approximately 200 μL for GC-MS analysis. The GC-MSD (Agilent GC 6890 N coupled with 5975C MSD, equipped with DB5-MS column, 30 m × 0.25 mm × 0.25 μm) had helium as carrier gas. The GC operating procedure was as follows: the sample was held at 60 °C for 2 min, ramped to 290 °C at 3 °C/min and held for 20 min. The sample was injected split-less with the injector temperature at 290 °C. The post-run time was 5 min with oven temperature at 310 °C.

G. PMF modeling

PMF is a multivariate factor analysis tool [7] that has been widely used for the source apportionment of atmospheric pollutants. $PM_{2.5}$ Sources were apportioned by using US EPA PMF 5.0 receptor model in our study. The PMF 5.0 program is described in detail by EPA PMF 5.0 Fundamentals & User Guide (http://www.epa.gov/heasd/research/pmf.html). Briefly, time series of chemical species can be viewed as a data matrix X with *i* by *j* dimensions, where *i* and *j* are the number of samples and chemical components measured, respectively. The objective of PMF is to solve the mass balance between the chemical species concentrations and the source profiles, as shown in Equation 1, with *p* number of factors, the species profile *f* of each source, and the amount of mass *g* contributed by each factor to each individual sample:

$$x_{ij} = \sum_{k=1}^{p} g_{ik} f_{kj} + e_{ij}$$

(1)

where e_{ij} is the residual concentration for each observation.

Results are obtained using the constraint that no sample can have significantly negative source contributions. PMF seeks a solution that minimizes the object function, Q, based upon the uncertainty for each observation, defined as follows:

$$Q = \sum_{i=1}^{n} \sum_{j=1}^{m} \left(\frac{e_{ij}}{u_{ij}} \right)^2$$

(2)

where u_{ij} is the measurement of uncertainty in the data point x_{ij}.

H. $PM_{2.5}$ stock suspensions preparation

The membranes were cut into 1 cm^2 pieces and sonicated for 1 h in dichloromethane/hexane followed by methanol [8]. Then, the suspensions were dried under N_2 gas and stored at -20°C. Before use, $PM_{2.5}$ was prepared with sterile cell cultures to a certain concentration and stored at 4°C.

I. RNA isolation and quality control

$PM_{2.5}$ samples were diluted in cell culture medium and added to cultures of BEAS-2B cells at the concentration of 100 μg/mL. Total RNA from lysed BEAS-2B cells was obtained using TRIzol followed manufacturer's instructions [9]. A NanoDrop (thermo) spectrophotometer was used to quantify the RNA concentration. Then, 500 ng of RNA was electrophoresed on an agarose gel. The RNA was stored at -80°C.

J. Gene expression Profiling and data analysis

An RNA library was constructed and sequenced using HiSeq 2500 SBS. Dysregulated pathways and dysregulated genes related these pathways were analyzed using the KEGG database and the GO database [9,10]. The human reference genome assembly used for alignment is GRCh38. Trim Galore software (http://www.bioinformatics.babraham.ac.uk/projects/trim_galore/) was used to control the quality of the method and the sequencing, Tophat software[11] was adopted for sequence alignment. For each sample, gene and transcript expressions were analyzed through Cufflink. After the normalization read counts for RNA through the library size, sequencing depth and gene length differences, Cuffdiff software was adopted for the differential analysis for each pair of comparison groups[12]. The differential

expression (cutoff value) between two transcripts was defined as greater than 2 fold (log2 ratio >1) with P-value less than 0.05. Multiple comparisons were taken into account for differentially expressed genes and pathway enrichment, with a false discovery rate of less than 5%（FDR≤0.05）. We analyze the pathway databases through the website (the link of www.genome.jp/kegg/pathway.html，1/15/2015).

K. Protein microarray preparation

The antibodies (rabbit antihuman NF-κB antibody, rabbit antihuman HO-1 antibody, rabbit antihuman NQO1 antibody, rabbit antihuman phospho-SAPK/JNK antibody, rabbit antihuman Nrf2 antibody, rabbit antihuman P53 antibody, rabbit antihuman MDM2 antibody, rabbit antihuman AKT1 antibody, rabbit antihuman FGFR1 antibody, rabbit antihuman FGF14 antibody, rabbit antihuman TNF-α antibody, rabbit antihuman caspase 1 antibody, rabbit antihuman IL-6 antibody, and rabbit antihuman IL-1β antibody) were diluted with PBS (pH 7.4) to 0.75 mg/mL. Aliquots were loaded onto 384-well plates (10μL/well) and spotted onto coated slides with a microarray printer (Capital Bio Co., Ltd., China) with array spotting pins. The delivery volume of the pin was approximately 100 pL. All samples were spotted in triplicate, and the final results were the average of the three samples. Mouse antihuman HO-1 antibody and goat antihuman NQO1 antibody diluted to 1 and 0.5 mg/mL were used as references to correct differences among the immunodetection chips. The spotted chips were kept at 37°C for 1 h and stored at -80°C [13].

L. Microfluidic device fabrication

The microfluidic chip had three layers, including the flow layer, the control layer and a glass substrate. The chips were fabricated using soft lithography [14,15]. AZ-50XT (AZ Electronic Materials.) photoresist was coated onto silicon to a thickness of 25 μm and patterned by exposure to UV light through a mask to form a mold. For the flow layer of cell culture chip and the control layer of the immunodetection chip, polydimethylsiloxane (PDMS) (RTV 615A and B in a 5: 1 ratio) was mixed and poured onto the molds. Before curing at 80°C for 1 h, PDMS was degassed for 1 h in a vacuum pump. Concurrently, the control layer of the cell culture chip and the fluidic layer of immunodetection chip were made by coating PDMS (A and B in a 20: 1 ratio) on the mold at 2000 rpm and baking at 80°C for 1 h. Then, the two layers were glued together and cured at 80°C for 1 h. Finally, the cell culture chip and the bonded flow and control structure were placed on a PDMS (A and B in a 20:1 ratio) coated glass slide and incubated at 80°C for at least 1 h. The chips were sterilized at 121°C for 30 min and then dried at 80°C before utilization. For the immunodetection chip, the bonded flow and control structure was precisely aligned onto a spotted microarray chip. The round reaction chambers of the microfluidic chip precisely covered the microarray. The aligned immunodetection chip was clamped lightly between two polymethylmethacrylate (PMMA) plates to prevent the microfluidic chip from separating during the experiment (Figure 1B).

M. Microfluidic cell culture

The human lung epidermal cell line BEAS-2B was cultured in BEBM medium with 100 U/ml penicillin and 100μg/ml streptomycin in a humidified incubator under 5% CO_2 at 37°C. The BEAS-2B cells were cultured for at least two weeks in flasks before the microfluidic experiments. Attached BEAS-2B cells were dissociated from the flasks with 0.25% trypsin-EDTA. Suspended BEAS-2B cells at a density of 10^7 cells mL^{-1} in BEBM were loaded into the cell culture chamber. Then, the microfluidic device was placed in an incubator with at 95% humidity, 5% CO_2 at 37°C for 24 h to promote cell attachment and growth.

N. Dilution network microfluidic operation

The fluid flow rate was 0.1μL min^{-1} for each gradient network unit. $PM_{2.5}$ was suspended in culture medium at concentrations of 100 μg/ml and 0μg/ml, and these suspensions were infused into the device simultaneously. Six continuous outlet concentrations (100, 80, 60, 40, 20, 0 μg/ml) were produced to determine the best performance.

O. Cell stimulation with $PM_{2.5}$

A gradient concentrations of $PM_{2.5}$ stimulated the cells, After a 24 h exposure, and lysis buffer was pumped into the cell culture chambers. Lysed cells were pumped out of the cell chambers and collected for ELISA to measure HO-1, P-JNK and MDM_2 proteins. The results showed that the optimal concentration of $PM_{2.5}$ was 60 μg/ml and consist with the results of immunodetection chip. Then, 60 μg/ml $PM_{2.5}$ was pump to the microfluidic chip. After 24 h exposure, lysis buffer and trypsin-EDTA

buffer were pumped into separate cell culture chambers. The lysed cells were infused to the downstream immunodetection chip. The dissociated cells were pumped out of the microfluidic chip for flow cytometry detection.

P. Immunodetection chip operation

Schematic illustrations of the protein immunoassay are shown in Figure S3. The operation was carried out as follows. Blocking buffer (120 μL) was loaded into the round reaction chambers (volume of each reaction chamber = 1.25μL) (Figure S3A), and the chip was then placed in an incubator at 37°C for 1hour. This blocking buffer incubation was performed to reduce background detection. Four linkage valves were closed to prevent cross-contamination of protein lysates from different samples. Protein lysates and cell culture supernatant (10μL) were pumped into separate round reaction chambers, and the valves were closed (Figure S3B). After incubation for 1 hour, washing buffer (PBST) was pumped into the chambers to rinse the samples (see Figure S3C). Stable coupling of primary antibodies (a mix of mouse antihuman NF-κB p65 antibody, mouse antihuman HO-1 antibody, mouse antihuman NQO1 antibody, mouse antihuman phospho-SAPK/JNK antibody, mouse antihuman Nrf2 antibody, mouse antihuman P53 antibody, and mouse antihuman caspase 1 antibody; a mix of mouse antihuman TNF-α antibody, mouse antihuman IL-6 antibody, mouse antihuman IL-1β antibody; and a mix of goat antihuman MDM2 antibody, and goat antihuman AKT1 antibody, goat antihuman FGFR1 antibody, goat antihuman FGF14 antibody, and goat antihuman VEGFA antibody) (Figure S3D), which were diluted 1:350 in PBST, were pumped into chip, and the device was placed in an incubator at

37°C for 1 hour. After incubation, the chambers were rinsed with washing buffer (Figure S3E). Secondary antibodies (donkey antigoat IgG cy3 conjugated and antimouse IgG Alxa555 conjugated) were diluted (1:1000 in PBST) and loaded (120μL) (Figure S3F). The whole microfluidic device was kept at 37°C for 1 hour. The chambers were then rinsed with washing buffer and double-distilled H_2O (Figure S3G). The valves of the microfluidic system were precisely operated using homemade digital solenoid valves driven by a relay board; this system was connected to a computer through a digital I/O. The microarray slides were dried by centrifugation (200rpm, 5 min) and then scanned in a microarray scanner (luxscan-10K/A) with a 532 nm source for Alxa555 and cy3. The signal intensity was measured, and the data were analyzed using the software accompanying the scanner (Figure S3H).

Q. ELISA

HO-1 protein levels were measured using ELISA to validate the results of Immunodetection chip. BEAS-2B cells were exposed to $PM_{2.5}$ for 24 hours, the culture medium was moved, and the cells were lysed using lysis buffer and tested by ELISA [16].

R. Cellular staining with fluorescent dyes and flow cytometer

The following dyes were added separately to dissociated cells and incubated at 37°C for 10-30 min: (1) 5 μM (DCFH-DA)(cytoplasmic reactive oxygen species generation); (2) 5 μM MitoSOX Red (mitochondrial reactive oxygen species generation); (3) 4 μM FLOU-3 (cytoplasmic free calcium production); (4) Annexin V-FITC/PI (assessment of cell apoptosis). Flow cytometry was performed using a

Gallios (Beckman Coulter, America) cytometer equipped with three argon lasers (488 nm, 638 nm, and 405 nm). DCF, FLOU-3, and Annexin V-FITC were analyzed in the FL-1 channel, while FL-2 was used to analyze MitoSOX Red fluorescence, and PI fluorescence was analyzed using the FL-3 channel [17,18].

S. TEM

For TEM, BEAS-2B cells cultured in 24-well plates were exposed to 100 μg/mL $PM_{2.5}$ for 24 h. Then, the cells were fixed with 2.5% glutaraldehyde in 0.1 M cacodylate buffer (pH 7.3) containing 2% sucrose at room temperature for 20 min and then with 1% OsO4 in 0.1 M cacodylate buffer (pH 7.3) for 30 min. The cells were then dehydrated using an ethanol gradient and cut with an Ultramicrotome (Leica, Stuttgart, Germany). Then, 200-mesh copper grids were stained with lead citrate and uranyl acetate, and the samples were analyzed by a Tecnai G2 20 TWIN transmission electron microscope [18,19].

2. Supplementary Reference

(1) Fengwen, W.; Tian, L.; Jialiang, F.; Huaiyu, F.; Zhigang, G. *Environ. Sci.: Process Impacts* **2014**, *17*, 197-205.

(2) Huang, K.; Zhuang, G.; Lin, Y.; Wang, Q.; Fu, J. S.; Fu, Q.; Liu, T.; Deng, C. *Atmos. Chem. Phys.* **2013**, *13*, 5927-5942.

(3) Yuan, H.; Wang, Y.; Zhuang, G. S. *J. Instrumental Anal.* **2003**, *22*, 11-14.

(4) Guo, L.; Chen, Y.; Wang, F.; Meng, X.; Xu, Z.; Zhuang, G. *Mar. Chem.* **2014**, *163*, 19-27.

(5) Chow, J. C.; Watson, J. G.; Pritchett, L. C.; Pierson, W. R.; Frazier, C. A.; Purcell, R. G. *Atmos. Environ.* **1993**, *27*, 1185-1201.

(6) Mai, B.; Qi, S.; Zeng, E. Y.; Yang, Q.; Zhang, G.; Fu, J.; Sheng, G.; Peng, P.; Wang, Z. *Environ. Sci. Technol.* **2003**, *37*, 4855-4863.

(7) Paatero, P.; Tapper, U. *Environmetrics* **1994**, *5*, 111-126.

(8) Fukagawa, N. K.; Li, M.; Poynter, M. E.; Palmer, B. C.; Parker, E.; Kasumba, J.; Holmén, B. A. *Environ. Sci. Technol.* **2013**, *47*, 12496-12504.

(9) Libalova, H.; Uhlirova, K.; Klema, J.; Machala, M.; Sram, R. J.; Ciganek, M.; Topinka, J. *Part. Fibre. Toxicol* **2012**, *9*, 1-16.

(10) Ding, X.; Wang, M.; Chu, H.; Chu, M.; Na, T.; Wen, Y.; Wu, D.; Han, B.; Bai, Z.; Chen, W.; Yuan, J.; Wu, T.; Hu, Z.; Zhang, Z.; Shen, H. *Toxicol. Lett.* **2014**, *228*, 25-33.

(11) Trapnell, C.; Pachter, L.; Salzberg, S. L. *Bioinformatics* **2009**, *25*, 1105-1111.

(12) Trapnell, C.; Hendrickson, D. G.; Sauvageau, M.; Goff, L.; Rinn, J. L.; Pachter, L. *Nat. Biotechnol.* **2013**, *31*, 46-53.

(13) Jiang, X.; Shao, N.; Jing, W.; Tao, S.; Liu, S.; Sui, G. *Talanta* **2014**, *122*, 246-250.

(14) Lee, C. C.; Sui, G.; Elizarov, A.; Shu, C. J.; Shin, Y. S.; Dooley, A. N.; Huang, J.; Daridon, A.; Wyatt, P.; Stout, D. *Science* **2005**, *310*, págs. 1793-1796.

(15) Jing, W.; Zhao, W.; Liu, S.; Li, L.; Tsai, C. T.; Fan, X.; Wu, W.; Li, J.; Yang, X.; Sui, G. *Anal. Chem.* **2013**, *85*, 5255-5262.

(16) King, E. M.; Vailes, L. D.; Tsay, A.; Satinover, S. M.; Chapman, M. D. *J Allergy Clin Immunol* **2007**, *120*, 1126-1131.

(17) Xia, T.; Korge, P.; Weiss, J. N.; Li, N.; Venkatesen, M. I.; Sioutas, C.; Nel, A. *Environ. Health Perspect.* **2004**, *112*, 1347-1358.

(18) Xia, T.; Kovochich, M.; Brant, J.; Hotze, M.; Sempf, J.; Oberley, T.; Sioutas, C.; Yeh, J. I.; Wiesner, M. R.; Nel, A. E. *Nano lett.* **2006**, *6*, 1794-1807.

(19) Nel, A. *Science* **2005**, *308*, 804-806.

3. Supplementary Figures and Tables

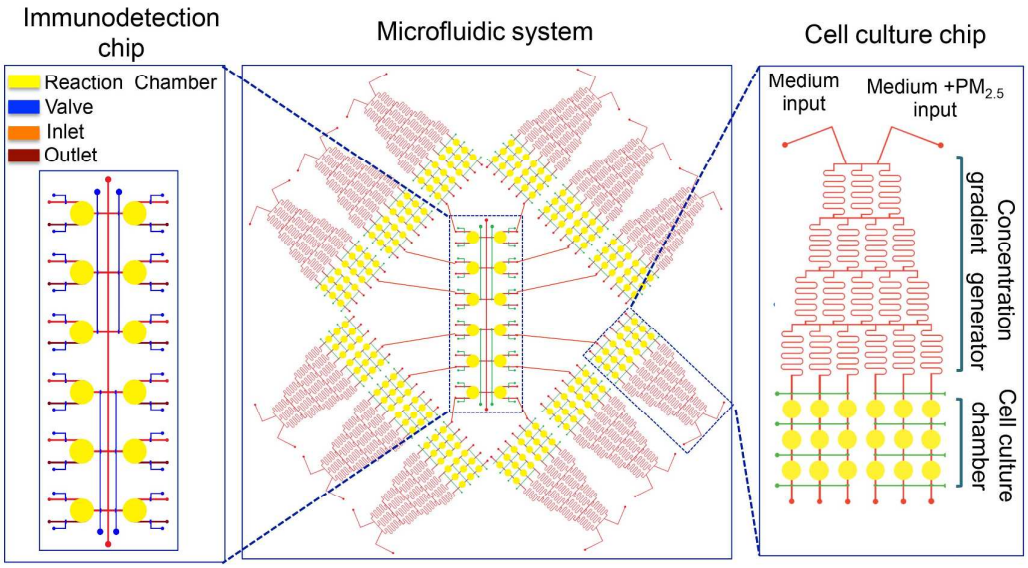

Figure S1. Schematic of the microfluidic system for cellular toxicity induced by $PM_{2.5}$. The microfluidic system consists of twelve uniform structures and an immunodetection chip. The single structure unit containing the concentration gradient generator (CGG) is magnified.

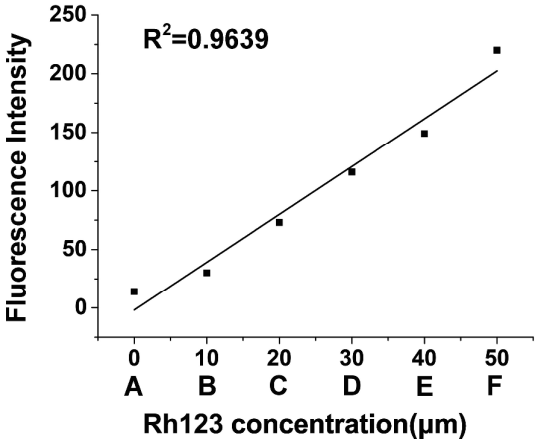

Figure S2. Experimentally collected data and theoretical calculations were compared for the dilution network.

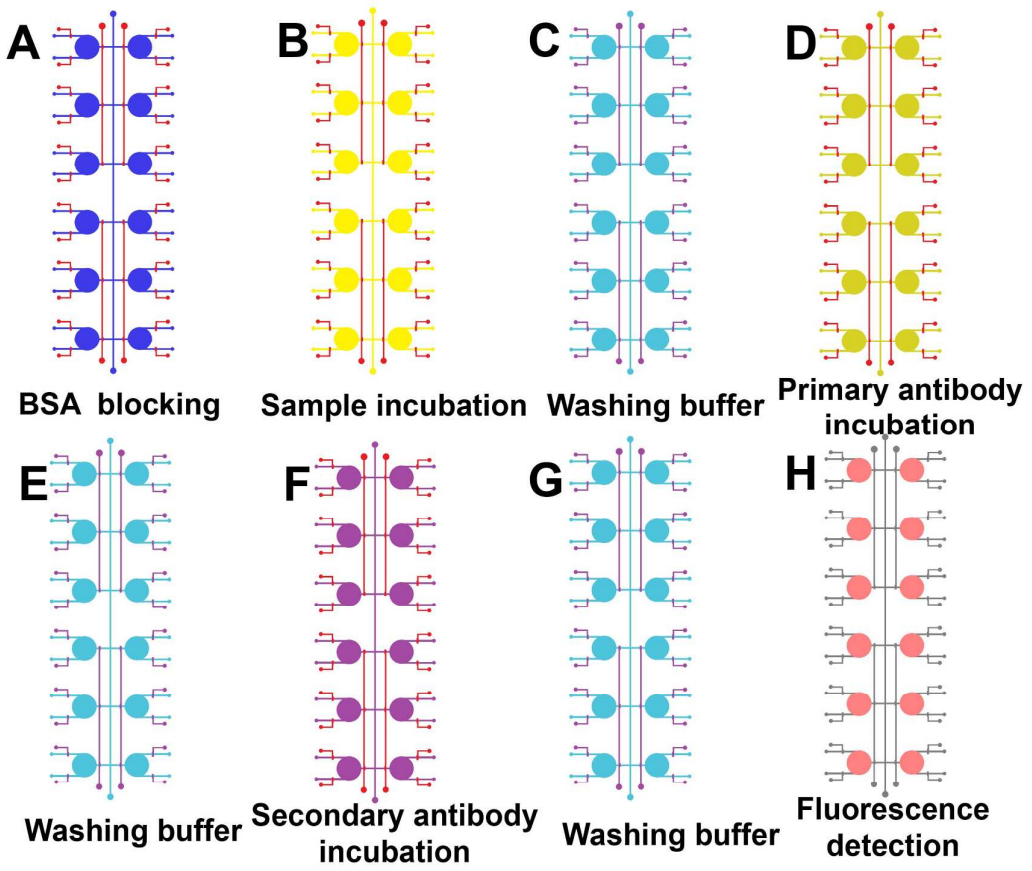

Figure S3. Illustration of the immunodetection chip operation for the protein immunoassay. The red valves indicate that the valve is closed; purple valves indicate that the valve is open. (A) Blocking buffer was loaded into the round reaction chambers. (B) Samples were pumped into separate round reaction chambers and then the chip was incubated for 1 hour. (C) PBST was pumped into the chambers to rinse. (D) Stable coupling of primary antibodies. (E) The chambers were rinsed with PBST. (F) Secondary antibodies were loaded. (G) The chambers were rinsed with PBST and double-distilled H_2O. (H) The microarray slides were scanned in a microarray scanner.

Genes/Proteins	$PM_{2.5}$ dose[a]	RNA-seq	$PM_{2.5}$ dose[b]	Chip	Related pathway
NAD(P)H: quinone oxidoreductase 1(NQO1)	80		60		Nrf2/ARE signaling pathway
Heme oxygenase 1 (HO-1)	80		60		Nrf2/ARE signaling pathway
Nuclear factor erythroid-2-related factor 2 (Nrf2)	80		60		Nrf2/ARE signaling pathway
Interleukin 1 beta (IL-1β)	80		60		NF-κB cascade
Caspase 1 (CASP1)	80		60		NF-κB cascade
Nuclear factor kappa B (NF-κB)	80		60		NF-κB cascade
Tumor necrosis factors alpha (TNF-α)	80		60		NF-κB cascade
C-Jun NH2- terminal kinases (JNK)	80		60		MAPK pathway
Interleukin 6 (IL-6)	80		60		JAK-STAT pathway
Serine/threonine-protein kinases1 (AKT1)	80		60		P13-AKT signal transduction
Fibroblast growth factor 14 (FGF14)	80		60		cytokine-cytokine receptor interaction
FGF receptor (FGFR1)	80		60		cytokine-cytokine receptor interaction
Vascular endothelial growth factor (VEGFA)	80		60		VEGF signaling pathway
Mouse double minute 2 homolog (MDM2)	80		60		P13-AKT signal transduction
P53	80		60		P13-AKT signal transduction
Wingless-type family member 5A (WNT5A)	80				Wnt signaling pathway
T-cell factor/lymphoid enhancer factor (TCF/LCF)	80				Wnt signaling pathway

Signal Transducer And Activator Of Transcription 5A (STAT5A)	80				JAK-STAT pathway
Caspase 3 (CASP3)	80				Pathways in cancer
B-cell lymphoma 2 (BCL-2)	80				Regulation of release of cytochrome c from mitochondria
Transforming growth factor beta receptor (TGFβR)	80				Endocytosis
Caveolin1 (CAV1)	80				Endocytosis
Dynamin2 (DNM2)	80				Endocytosis
Dynamin3 (DNM3)	80				Endocytosis

Figure S4. Genes and proteins invloved in selected deregulated pathways from BEAS-2B cells exposed to $PM_{2.5.}$ Red : upregulation; Green : downregulation; Yellow : regulation; Blue: chip verification undone. [a] $PM_{2.5}$ dose: 80 μg/mL; [b] $PM_{2.5}$ dose: 60 μg/mL.

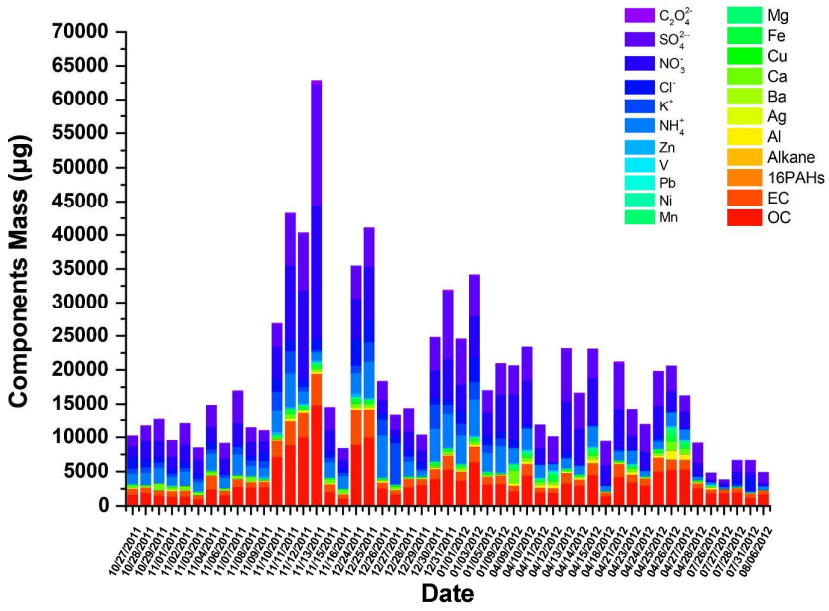

Figure S5. Daily concentration of 22 chemical components of $PM_{2.5}$ during four seasons from 27 October in 2011 to 14 August in 2012.

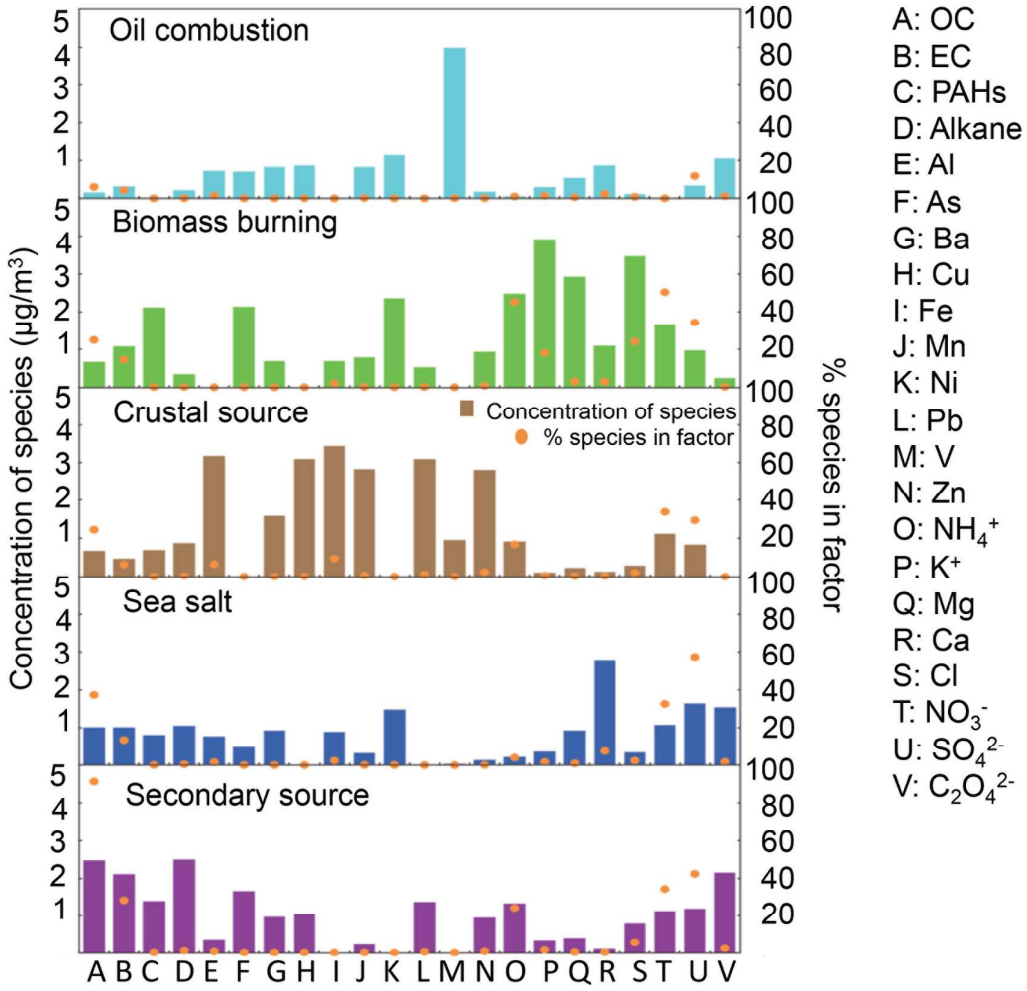

Figure S6. Five factor loadings by PMF analysis from 49 $PM_{2.5}$ samples collected in Shanghai over four seasons.

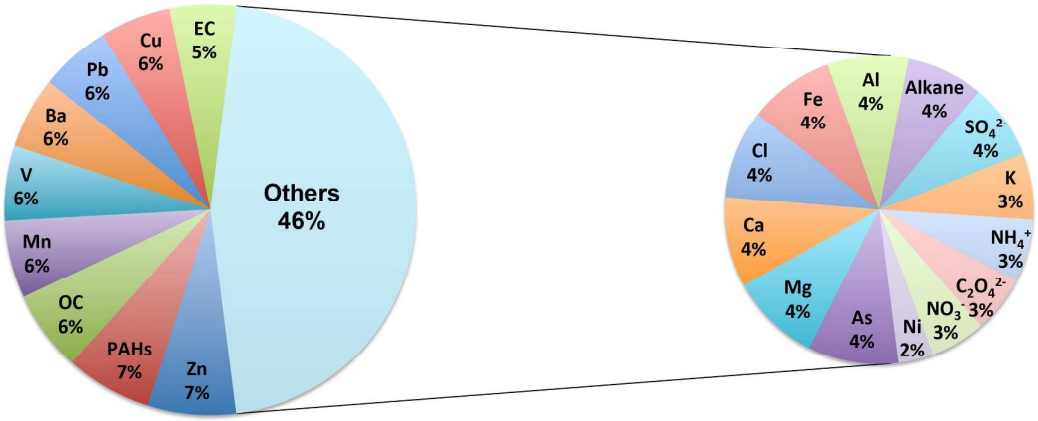

Figure S7. Contributions of the 22 chemical components of $PM_{2.5}$ on 15 measured dysregulated proteins over four seasons.

Table S1: KEGG pathways significantly dysregulated after $PM_{2.5}$-treatment of BEAS-2B cells.

KEGG pathway	Genes	P-value
Pathways in cancer	MMP2, BMP4, CBLB, CASP3, MMP1, AKT1, MDM2, XIAP, TGFBR1, FGF14, RALGDS, PML, LAMA4, FGFR1, WNT5A, TFG, MSH6, TCF7L2, MLH1, STAT5A, EGLN2, VEGFA	0.000810528
Endocytosis	CBLB, ZFYVE9, SMAP1, DAB2, CAV1, DNM1, MDM2, SMAP2, IL2RG, TGFBR1, DNM2, RUFY1, PML, PSD3, DNM3, NEDD4L	0.000923386
Measles	TNFSF10, CBLB, EIF2AK3, AKT1, IL2RG, IFNGR2, MAVS, IRAK4, IFNAR2, IFNGR1, STAT5A, TNFAIP3	0.001511923
Colorectal cancer	CASP3, AKT1, TGFBR1, RALGDS, MSH6, TCF7L2, MLH1	0.004531177
Bladder cancer	MMP2, TYMP, MMP1, MDM2, VEGFA	0.008493859
Folate biosynthesis	GCH1, FPGS, DHFR	0.010602013
Hippo signaling pathway	BMP4, FBXW11, DLG1, CTGF, TGFBR1, ID1, WWC1, PPP2R2B, ID2, WNT5A, TCF7L2	0.013744386
Cytokine-cytokine receptor interaction	CXCL6, TNFSF10, INHBE, IL7R, IL17RA, IL2RG, TGFBR1, IFNGR2, CTF1, CCL20, IFNAR2, IL1RAP, IFNGR1, LEPR, VEGFA	0.02483671
One carbon pool by folate	SHMT1, DHFR, MTR	0.024875097
Jak-STAT signaling pathway	CBLB, IL7R, AKT1, IL2RG, IFNGR2, CTF1, IFNAR2, IFNGR1, STAT5A, LEPR	0.03549342
Herpes simplex infection	EIF2AK3, CASP3, IFNGR2, ARNTL, TBP, PML, SP100, MAVS, IFNAR2, IFNGR1, POLR2A	0.03828124
Bacterial invasion of epithelial cells	CBLB, CAV1, DNM1, CTTN, DNM2, DNM3	0.04168585

Table S2: GO pathways significantly dysregulated after $PM_{2.5}$-treatment of BEAS-2B cells.

GO Pathway	Genes	P-value
Cellular response to chemical stimulus	LTBP4, HMOX1, MMP2, CORO1A, ECT2, IGFBP5, EREG, BMP4, GDF15, STC2, ZFYVE9, PRKD2, VCAM1, ZNF35, TSC1, IL7R, EIF2AK3, CASP3, UCP2, IL17RA, DAB2, CEP57, MEF2A, CAV1, ATP7A, FOXO3, AKT1, MDM2, MYO5A, SAA1, HYAL3, RUNX2, CTGF, GFRA1, PDE4B, ANKRD1, COL16A1, IL2RG, TGFBR1, ID1, FGF14, NQO1, SFRP1, CDKN1C, IFNGR2, EIF4E3, RHBDD1, PML, NUP50, PDE1C, ID2, GRB10, SP100, MAVS, FGFR1, SLC29A1, GNB2, IRAK4, TRIM5, IFNAR2, IL1RAP, PAPSS2, UMPS, WNT5A, ATP6V0E2, COL6A1, SLIT2, PKD2, NUP54, ADD1, SLIT3, LYN, CASP1, NUP107, MTR, FBN1, TRAP1, LRP6, TCF7L2, IFNGR1, NCEH1, AK4, VDR, NFATC4, ATP6V1D, GREM1, BAIAP2, NEDD4L, PIN1, STAT5A, LONP1, EGLN2, UBA52, CYP1B1, TNFAIP3, LEPR, PRKD1, VEGFA	0.00000307
Response to organic substance	LTBP4, HMOX1, MMP2, CORO1A, IGFBP5, EREG, BMP4, GDF15, GCH1, STC2, HNMT, GJA1, ZFYVE9, PRKD2, VCAM1, ZNF35, TSC1, IL7R, EIF2AK3, CASP3, UCP2, IL17RA, SCAP, DAB2, CEP57, MEF2A, CAV1, FOXO3, HDAC4, AKT1, XRCC3, KCNMA1, MDM2, MYO5A, HYAL3, RUNX2, RBBP5, CTGF, GFRA1, PDE4B, ANKRD1, COL16A1, DKK1, IL2RG, TGFBR1, ID1, FGF14, NQO1, CD83, SFRP1, CDKN1C, IFNGR2, EIF4E3, RHBDD1, SERPINA1, PML, BDNF, NUP50, PDE1C, ABCG1, GRB10, SP100, UQCRC1, MEST, MAVS, FGFR1, SLC29A1, GNB2, IRAK4, TRIM5, IFNAR2, IL1RAP, WNT5A, ATP6V0E2, COL6A1, GDAP2, SLIT2, DHFR, LOX, NUP54, ADD1, SLIT3, LYN, CASP1, NUP107, FBN1, LRP6, TCF7L2, IFNGR1, VDR, ATP6V1D, BAIAP2, TRIM16, NEDD4L, PIN1, STAT5A, LONP1, UBA52, TNFAIP3, LEPR, PRKD1, VEGFA, DGKD	0.00000728
Response to oxygen levels	HMOX1, MMP2, STC2, VCAM1, UCP2, SCAP, CAV1, AKT1, KCNMA1, MDM2, CTGF, ANKRD1, SFRP1, SERPINA1, PML, BDNF, SLC29A1, SCFD1, CASP1, LONP1, EGLN2, UBA52, VEGFA	0.0000102

Negative regulation of transmembrane receptor protein serine/threonine kinase signaling pathway	ZFYVE9, BMPER, CAV1, DKK1, TGFBR1, SFRP1, WNT5A, FBN1, TCF7L2, GREM1, NEDD4L, PIN1, UBA52	0.0000254
	ECT2, TNFSF10, BMP4, GCH1, IER3, APBB2, CASP3, MEF2A, FOXO3, AKT1, KCNMA1, ANKRD1, TGFBR1, ARHGEF7, NQO1, SFRP1, UACA, DNM2, PPP2R2B, PML, PPP2R4, WNT5A, SLIT2, LYN,	
Positive regulation of apoptotic process	CASP1, LRP6, TCF7L2, VDR, NFATC4, IGFBP3, BCL2L11	0.0000842
Positive regulation of endothelial cell chemotaxis by VEGF-activated vascular endothelial growth factor receptor signaling pathway	PRKD2, PRKD1, VEGFA	0.00016
	HMOX1, ECT2, TNFSF10, FBXW11, GJA1, UACA,	
Regulation of I-kappaB kinase/NF-kappaB cascade	ZMYND11, MAVS, ATP2C1, TRIM5, TFG, CASP1, GREM1, CC2D1A, UBA52, TNFAIP3, PRKD1	0.000417
Interleukin-7 receptor activity	IL7R, IL2RG	0.00122
Wnt receptor signaling pathway involved in somitogenesis	DKK1, SFRP1, LRP6	0.0013
	RB1CC1, BMP4, PRKD2, BMPER, DAB2, MEF2A, CAV1, AKT1, RGS4, CTGF, TGFBR1, MAP3K8, ID1, FGF14, SFRP1, ZMYND11, CAMKK2, WWC1, FGFR1, IRAK4, TRIM5, WNT5A, LYN, RBM4, DAG1, ROR2, GREM1, PIN1, UBA52, MAPK8IP3, IGFBP3,	
MAPK cascade	LEMD2, VEGFA, JNK	0.00162
Positive regulation of interleukin-1 secretion	SAA1, WNT5A, CASP1, TRIM16	0.00293
Regulation of inositol 1,4,5-trisphosphate-sensitive calcium-release channel activity	MYO5A, PKD2	0.0035
Negative regulation of toll-like receptor 2 signaling pathway	LYN, TNFAIP3	0.0035
	RB1CC1, DAB2, MEF2A, AKT1, CTGF, FGF14, SFRP1, ZMYND11, IRAK4, WNT5A, RBM4, ROR2,	
Stress-activated MAPK cascade	GREM1, UBA52, MAPK8IP3, VEGFA, JNK	0.00365
Regulation of release of cytochrome c from mitochondria	TNFSF10, AKT1, BMF, DNM1L, BCL2L11	0.0045
	RB1CC1, DAB2, AKT1, CTGF, FGF14, SFRP1, ZMYND11, IRAK4, WNT5A, ROR2, UBA52,	
JNK cascade	MAPK8IP3, JNK	0.0158
Interleukin-2 production	PRKD2, CD83, IL1RAP, STAT5A, TNFAIP3	0.0225

Response to DNA damage stimulus	HMOX1, POLM, IER3, NACC2, CASP3, FOXO3, XRCC3, MDM2, RBBP5, XIAP, ANKRD1, SMC1A, UACA, PML, INO80, SP100, FANCD2, NABP1, EYA2, NEK1, LYN, UVRAG, GTF2H1, MSH6, MLH1, TDG	0.0423